

# Local sensitivity analysis of a closed-loop *in silico* model of the human baroregulation.

Karolina Tlalka<sup>1,2</sup>[0009–0005–4575–3510], Harry Saxton<sup>3</sup>, Ian Halliday<sup>2,5</sup>, Xu Xu<sup>4,5</sup>[0000–0002–9721–9054], Daniel Taylor<sup>2,5</sup>, Andrew Narracott<sup>2,5</sup>, and Maciej Malawski<sup>1</sup>[0000–0001–6005–0243]

<sup>1</sup> Sano Centre for Computational Medicine, Nawojki 11, 30-072 Kraków, Poland

[k.tlalka@sanoscience.org](mailto:k.tlalka@sanoscience.org)

<https://sano.science/>

<sup>2</sup> Division of Clinical Medicine, School of Medicine and Population Health, University of Sheffield, Sheffield, United Kingdom

<sup>3</sup> Materials and Engineering Research Institute, Sheffield Hallam University, Howard Street, Sheffield, S1 1WB, United Kingdom

<sup>4</sup> Department of Computer Science, University of Sheffield, Sheffield, S1 4DP, United Kingdom

<sup>5</sup> Insigneo Institute for *in silico* Medicine, University of Sheffield, United Kingdom

**Abstract.** Using a minimal but sufficient closed-loop encapsulation and the theoretical framework of classical control, we implement and test the mathematical model of the baroregulation due to Mauro Ursino [24]. We present and compare data from a local relative sensitivity analysis and an input parameter orthogonality analysis from a regulated and then an equivalent unregulated cardiovascular model with a single ventricle and “CRC” Windkessel representation of the systemic circulation. We conclude: (i) a basic model of the closed-loop control is intrinsically stable; (ii) regulation generally (but not completely) suppresses the sensitivity of output responses on mechanical input parameters; (iii) with the sole exception of the regulation set-point, the mechanical input parameters are more influential on system outputs than the regulation input parameters. This work is the initial step for further analysis of more complex and computationally expensive models of the cardiovascular system, with baroreflex control, with possible applications in space-flight medicine or research on exercise intolerance.

**Keywords:** Baroreflex · Sensitivity Analysis · Digital Twin .

## 1 Introduction

The cardiovascular (CV) system is not an independent entity. Its function relies on external stimuli like posture shifts, exercise state and oxygen levels [2]. Blood pressure regulation is achieved by several long and short time-scale control mechanisms. The most important is the baroreflex [6]. A model incorporating a physiologically reasonable description within the framework of control theory, of the coupling with the CV system is critical to digital twin development. Such

a model would support a range of emerging applications - CV system response to gravitational acceleration, haemorrhage and arrhythmia (where experimental observation is challenging), to name a few.

The baroreflex is a short-term (seconds to minutes response) neurological mechanism, regulating blood pressure by adapting the CV system response, most importantly the heart period, ventricular contractility, venous tone, and systemic resistance [6]. We describe baroregulation within the framework of control theory [9], as a negative feedback problem. The feedback and feedforward elements form a single-input, multiple-output sub-system (Figure 1). Sensors (i.e., the baroreceptors) in the aortic arch and carotid sinus transduce mechanical strains to electrical signals which are transmitted via afferent nerves to the central nervous system. There, information is processed and a response signal is directed to local effectors, via sympathetic (“fight-or-flight”) and parasympathetic (“rest-and-digest”) nerves.

Several models of the baroreflex exist [7, 8, 17, 24]. The Ursino model [24] represents the control system with succinct mathematical descriptions of particular neurological physiology. Ottesen et al. [17] present similar solutions - a simple, computationally inexpensive model with pressure changes as inputs for baroreflex function; also a more complex model with wider applications detailing down to nervous activity. Heldt et al. [7, 8] developed a more empirical approach, based on DeBoer’s earlier work [4] and making limited appeal to control theory concepts.

A model, a set of clinical hypotheses and an appropriate methodology should co-evolve. An initially parsimonious base model is advanced by increased complexity in some aspect of its function, motivated by a need to test particular hypothesis relating to, e.g. treatments, involving this function. A relevant example is the work of Gee et al. [5], where the authors evolve Ursino’s model [24], with Park et al.’s modifications [18], extending the model to describe the intrinsic cardiac nervous system, aiming to study respiratory sinus arrhythmia.

To understand baroreflex operation, an appropriate model of flow and biomechanics (termed a mechanical model) must be coupled with the regulation model and suitable test scenarios devised. Long scenario timescales and high computational costs militate for a reduction in dimensionality. Mechanical model complexity can be systematically reduced to one-dimensional (1D) formulations [13], e.g. to describe pulse-wave propagation phenomena, or further, to zero-dimensional (0D) formulations (also called lumped-parameter models) [22] which was the approach used in this work. A 0D formulation (Figure 2) was chosen because of the specificity and provenance of the baroreflex model available and used in this work [24], which provides lumped parameters values- no counterpart parameterisation is currently available (to our knowledge) in models with higher dimensionality. Because of this reduction, some output information was lost (e.g. arterial cross-sectional pressures and detailed flow patterns), but in this application such data are not essential. Advantages and weaknesses of the 0D method are described in [22].

Personalised medicine is focused on considered, substantive resource management [1, 25]. Personalisation is perhaps the central problem in the field, in which a model is calibrated to provide a digital representation of a specific patient. This task increases in difficulty with an increase in the number of input parameters and so it is desirable to minimise this number, under the constraint that key behaviours must emerge from the model. The mathematical tool that facilitates the study of the impact of changes in model inputs on model outputs - and the interaction between them - is sensitivity analysis (SA), for which there is an extensive literature in the context of medical applications [15, 16, 21]. Information from SA may be supplemented with orthogonality analysis [15]. By analysis of the significance and orthogonality of inputs, one can systematically identify a minimal subset of parameters, to be used in the personalisation task [16]; the simplified model is then said to have been *reduced*. The result of a model reduction depends of course upon one’s initial model.

We aim to assess the unmodified baroregulation model of Ursino [24] within: (i) a minimal but physiologically sufficient, closed-loop encapsulation and (ii) the framework of classical control theory. To achieve this, we perform local relative sensitivity analysis (LSA) using “one-at-the-time” (OAT) formulation and orthogonality analysis both of a regulated and an equivalent unregulated, model. The latter is defined as one with parameters  $R_{sys}$ ,  $E_{LVmax}$  and  $\tau_0$  set to the values emerging from the periodic state of that regulated model. This comparison quantifies any shift in the relative influence of model input factors on a chosen subset of discrete, derived outputs. See Figure 3. Interactions between parameters and higher-order effects are not considered in LSA- they are the subject of global sensitivity analysis (GSA) and future work. LSA was performed because of its simplicity, low computational cost and as a preliminary method in our investigations of regulated models, preceding a GSA. We return to this point in our Conclusions. While we are aware that LSA overlooks non-linear model properties, we assume, here, that in the periodic state (a physiological state of rest), the non-linear nature of the model will play only a negligible part, based upon findings with unregulated, purely mechanical models [19].

## 2 Methods

Here we describe our model formulation with emphasis on the baroreflex, we outline closed-loop simulations using the model and describe methods to perform a local relative sensitivity analysis and orthogonality analysis.

### 2.1 Baroreflex model

Ursino’s formulation [24] transparently represents key physiological functions. Formally, our baroreflex model is a set-point controlled closed-loop regulator. It is presented in the block diagram form in Figure 1. The Laplace transfer functions shown re-cast Ursino’s ordinary differential equation formulation. The associated mechanical model has a single ventricle representation (see Figure 2)

for which the formulation is reported elsewhere [3], [21]. These two sub-models were combined in ODE or state-space form [9] as follows:

$$\frac{d}{dt}\underline{P}(t; \underline{\theta}) = \underline{f}(\underline{P}; \underline{\theta}).$$

Above,  $\underline{P}(t; \underline{\theta})$  is a vector of compartmental pressure time series (or pressure surrogates [24], in the case of the control sub-system),  $\underline{\theta}$  is an input parameter vector and  $t$  is time. The ODE or state-space formulation of the cardiovascular model is mathematically described by Saxton et al., [21] and our baroreflex sub-model by Ursino [24].

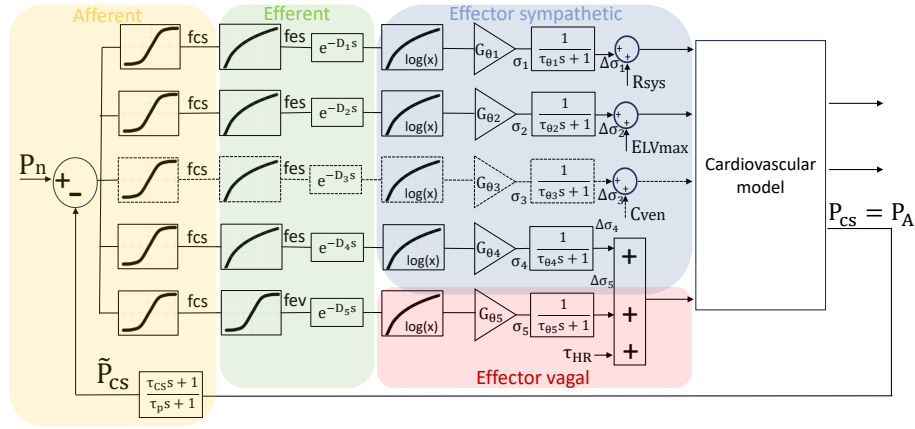
A single mechanical model output of aortic pressure (a surrogate for Ursino’s carotid sinus pressure), provides the input for the baroreceptor block and is compared to a pre-defined pressure set-point to evolve an error signal with units of pressure, a proxy for nervous electrical pulsation. The overall regulation algorithm drives central nervous system (CNS) and autonomic nervous system (ANS) regulatory responses, designed to minimise this error. This process has defined effector dynamics expressed here in the form of Laplace transfer functions. Note, signals from the effectors are superposed with a constant, base value of each system factors in the effectors’ evolution. This imparts an effective integral action to the control, as recognised by Heldt [8]. In fact, it may be shown to conform with integral action control such as that posited by Heldt et al.[8], complicated somewhat because of a presence of time delays with electro-physiological and biochemical origins. Our regulated CV model, described in section 2.2, was applied in a rest state (i.e. without any representation of a physiological perturbation). Regulation was applied from  $t = 0$  and:

1. no cycle-averaging or smoothing was necessary for stable results,
2. beat-to-beat sampling of cardiac control parameters after Heldt et al. [7] is required for a physiologically feasible and mathematically stable solution. Specifically, stable results are impossible when evolving regulation HR effectors for heart period continuously, as it is easy to show that period within a beat can cause *reduction* of the value  $\tau$ - which should increase monotonically. We update heart period and maximal ventricular elastance only at the beginning of a beat; systemic resistance was adjusted at every time step.

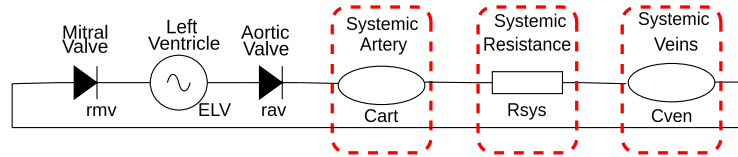
Input parameter values and associated sources (references) are summarised in Table 1.

## 2.2 Cardiovascular circulation model

To expose the operation of heart regulation, we choose to use the simplest feasible mechanical model, capable of exposing regulation phenomena. This simplicity allows one to uncover the structure and key details of the sensitivities’ of the baroreflex model, which is our main interest. Specifically, we use a 0D single ventricle model, with a Shi double cosine elastance function [12], coupled to a passive ‘‘CRC’’ Windkessel model, representing the systemic circulation; the latter is shown in electrical analogue form in Figure 2.



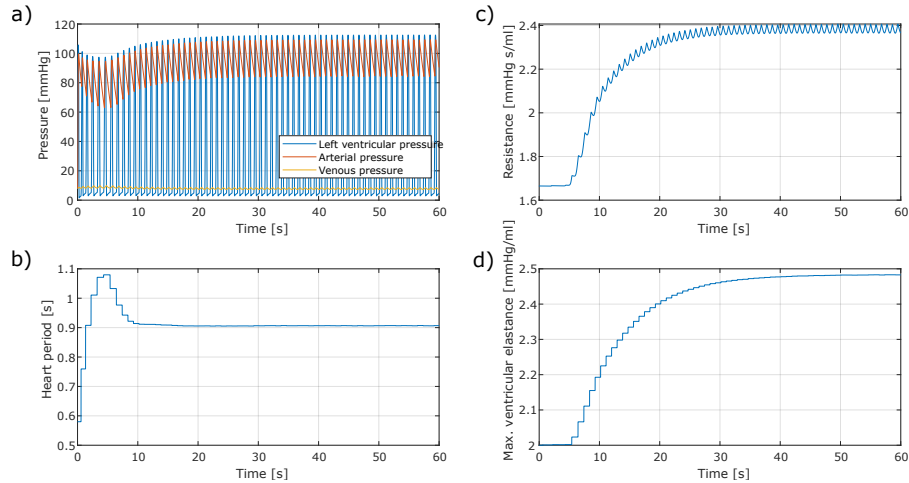
**Fig. 1.** Block diagram of our closed-loop baroreflex control mechanism [24]. The corresponding regulated mechanical model is represented in Figure 2. For the baroreceptors, the input is the carotid sinus pressure,  $P_{CS}$ , and the output is a surrogate pressure  $\tilde{P}_{CS}$  with units of spike-rate. The regulation set point, defined by Ursino as the pressure at the central point of the sigmoid describing carotid sinus pressure [24], is  $P_n$  (far left). Variables  $f_{cs}(t)$  (carotid sinus frequency),  $f_{es}(t)$  (efferent sympathetic frequency) and  $f_{ev}(t)$  (efferent vagal frequency) have units of spikes per second. The delay blocks can be commuted with the signal compression blocks and represent the cumulative effect of ANS and CNS processing. Solid colour blocks locate the control functions to afferent, efferent or organ nervous activity. Afferent processing is described by a first-order ODE with 2 time constants -a first order Laplace transfer function (LTF)- followed by a sigmoidal functional compression to describe the conversion spike rate. In the efferent arc, depending on the unit of spiking activity, the efferent frequency is calculated for the sympathetic (vagal) arc using an exponential (sigmoid) functional block. In the effectors (blue and red regions of the diagram) processing involves logarithmisation and multiplication by a particular gain factor and first-order LTF. Sympathetic and parasympathetic effector processing modulates the base values of the mechanical system input parameters: systemic resistance, ventricular contractility, venous compliance, sympathetic heart period and the vagal heart period. The change of the heart period is the effect of summation of the sympathetic and parasympathetic influence. Of course, blocks in the effector part can also be commuted.



**Fig. 2.** Our single ventricle, mechanical model in electrical analogue form. The elastance of the left ventricle,  $E_{lv}$ , is a Shi-double cosine model [12], which relates chamber pressure and volume. The valves are assumed to have Ohmic behaviour, under both forward and reverse bias, with the regurgitating resistance set very large. Our notation for the resistances (haemodynamic dissipation) and capacitances (vessel compliance) etc. and their numerical values are declared in Table 1.

**Table 1.** Parameter values of the unregulated CV system. Adapted from [21]. For the corresponding regulation and Windkessel parameters, see Table 3 of reference [24].

Parameters	Symbols	Values	Units	Sources
Mean circulatory filling pressure	$mcfp$	8.000	$mmHg$	Zucker et al. [26]
Heart period	$\tau_0$	0.580	$s$	Ursino [24]
Initial left ventricular volume	$V_{LV}$	160	$ml$	Kawel-Boehm et al. [11]
Minimal left-ventricular elastance	$E_{LVmin}$	0.060	$\frac{mmHg}{ml}$	Simaan et al. [23]
Maximal left-ventricular elastance	$E_{LVmax}$	2.000	$\frac{mmHg}{ml}$	Simaan et al. [23]
Time of systolic phase peak	$\tau_{S1LV}$	0.300	$s$	Björdalsbakke et al. [3]
Time of systolic phase end	$\tau_{S2LV}$	0.450	$s$	-
Aortic valve resistance	$r_{av}$	0.033	$\frac{mmHg \cdot s}{ml}$	Björdalsbakke et al. [3]
Mitral valve resistance	$r_{mv}$	0.060	$\frac{mmHg \cdot s}{ml}$	Björdalsbakke et al. [3]
Arterial compliance	$C_{art}$	1.130	$\frac{ml}{mmHg}$	Björdalsbakke et al. [3]
Systemic resistance	$R_{sys}$	1.663	$\frac{mmHg \cdot s}{ml}$	Kamoi et al. [10]
Venous compliance	$C_{ven}$	11.000	$\frac{ml}{mmHg}$	Björdalsbakke et al. [3]

**Fig. 3.** Time series simulation data: a) pressure time series; b) applied heart period changes, shown as a time series (the *quantised* form of this regulation effector is apparent); c) systemic vascular resistance (SVR) evolution time series (the continuous form of the SVR regulation is clear); d) maximum left ventricular elastance (chamber contractility) changes in time. Initially, as the system equilibrates, some fluctuations of regulated values are apparent; as the system enters a periodic state, significantly smaller changes of regulation parameters occur.

### 2.3 Sensitivity and Orthogonality Analysis

We perform LSA of the unregulated and the equivalent closed-loop regulated CV models to determine the relative influence of input parameters on the chosen derived outputs and to investigate the impact of regulation on system sensitivities, and input parameter orthogonality to determine which inputs influence outputs in a similar way.

**Local Relative Sensitivity Analysis** Although LSA represents a quasi-linearisation of input parameter effects about an operating point, a low computational cost means that LSA remains a canonical first step in understanding our model's input parameter effects to: (i) verify correct interaction between the CV and regulation models and (ii) identify the non-influential input parameters. Relative sensitivity matrices were calculated using a central difference method (equation 1), perturbing inputs one at a time, about a reference state  $\underline{\theta}_0$ :

$$s_{i,j} = 2 \left( \frac{X_j(t^*; \underline{\theta}^+) - X_j(t^*; \underline{\theta}^-)}{X_j(t^*; \underline{\theta}^+) + X_j(t^*; \underline{\theta}^-)} \right) \left( \frac{\theta_i}{\Delta \theta_i} \right). \quad (1)$$

Above,  $t^*$  represents a discrete sample time,  $X_j(t^*; \underline{\theta}^+)$  the  $j$ -th output with  $\theta_i \rightarrow (\theta_i + 0.5\Delta\theta_i)$  and  $X_j(t^*; \underline{\theta}^-)$  the  $j$ -th output with  $\theta_i \rightarrow (\theta_i - 0.5\Delta\theta_i)$ . In the simulation, there were 36 inputs required to describe both the CV and baroreflex models. See Table 1 for elastance and valve factors and Table 3 of Ursino [24] for the following regulation and Windkessel parameters. Perturbed parameters were:  $R_{sys}$ ,  $C_{art}$ ,  $C_{ven}$ ,  $\tau_0$ ,  $r_{av}$ ,  $r_{mv}$ ,  $\tau_{S1LV}$ ,  $\tau_{S2LV}$ ,  $E_{LVmax}$ ,  $E_{LVmin}$ ,  $P_n$ ,  $k_a$ ,  $f_{min}$ ,  $f_{max}$ ,  $\tau_z$ ,  $\tau_p$ ,  $f_{es,\infty}$ ,  $f_{es,0}$ ,  $f_{es,min}$ ,  $k_{es}$ ,  $f_{ev,0}$ ,  $f_{ev,\infty}$ ,  $f_{cs,0}$ ,  $k_{ev}$ ,  $G_{T,v}$ ,  $\tau_{T,v}$ ,  $D_{T,v}$ ,  $G_{T,s}$ ,  $\tau_{T,s}$ ,  $D_{T,s}$ ,  $G_{E_{max,lv}}$ ,  $\tau_{E_{max,lv}}$ ,  $D_{E_{max,lv}}$ ,  $G_{R,sp}$ ,  $\tau_{R,sp}$ ,  $D_{R,sp}$ . The heart period, compliance and systemic resistance of the base mechanical model were chosen so that the emergent, regulated state was a plausible representation of a normal individual (heart period = 0.58). For the LSA presented below, the above factors were varied by  $\pm 5\%$  and  $\pm 10\%$  from the reference values. Two cases are considered: the periodic steady-state with and without regulation. For parity, the unregulated model's parameterisation was chosen so that, as far as possible, the regulated and unregulated periodic states are matched. In the regulated model, we analysed the influence of **36 inputs** on the following **10 outputs**: minimal and maximal values of: left ventricular pressure, arterial pressure, venous pressure and left ventricular volume, and heart period and cardiac output. In the unregulated model, heart period is excluded from the outputs and the following **10 inputs** were considered  $R_{sys}$ ,  $C_{art}$ ,  $C_{ven}$ ,  $\tau_0$ ,  $r_{av}$ ,  $r_{mv}$ ,  $\tau_{S1LV}$ ,  $\tau_{S2LV}$ ,  $E_{LVmax}$  and  $E_{LVmin}$ .

**Orthogonality Analysis** A LSA helps to identify from the full input parameter list an optimal subset of inputs for use in model personalisation. Different optima exist. For example, one might select, using the criterion of influence, those model input parameters which, when changed, move the outputs the most. How-

ever, two input parameters which, when changed, displace all output metrics in a parallel direction cannot act together to increase the dimensionality of the output space explored- the personalisation subspace. To identify such redundancy between the action of inputs we define a convenient metric of the orthogonality between two input parameters, which is based upon the sensitivity vectors

$$\hat{S}_i = (s_{i,1}, s_{i,2}, \dots, s_{i,N_0}), \quad i \in [1, 36],$$

defined for each input parameter. Above,  $N_0 = 9$  (10) for the unregulated (regulated) system. This metric measures the displacement action about the base state, due to input  $i$ , across all outputs by comparing sensitivity vectors  $\hat{S}_i$  and  $\hat{S}_{i'}$ . Measure  $d_{i'i}$  is an inner product measure for the orthogonality between any two input parameters  $\theta_i$  and  $\theta_{i'}$

$$d_{i'i} = \sin \left[ \cos^{-1} \left( \frac{\hat{S}_{i'}^T \cdot \hat{S}_i}{\|\hat{S}_{i'}\| \|\hat{S}_i\|} \right) \right], \quad i, i' = 1, \dots, n, \quad d_{i'i} \in [0, 1], \quad (2)$$

Above,  $\|\cdot\|$  denotes the Euclidean norm and the sin function simply ensures that  $d_{i'i} \in [0, 1]$ . Following the work of Olsen et al. [14], the Fisher information matrix

$$\mathbf{F} = \mathbf{s} \cdot \mathbf{s}^T,$$

encapsulates the collective properties of influence and orthogonality of the sensitivity vectors,  $\hat{S}$ . Above,  $\mathbf{s}$  is the  $36 \times 10$  matrix with elements  $s_{ij}$ , see equation (1). By seeking both sensitive and orthogonal inputs, one can obtain an optimally effective set of inputs for model personalisation.

### 3 Results

The system was solved numerically using the MATLAB (The MathWorks, Inc., Natick, Massachusetts, USA) ode15s implicit Euler solver recommended for stiff differential equations (variable-order, variable-step method). The relative and absolute solver tolerance was  $1e^{-7}$  and maximum step size was 0.01. An output function, called at each iteration, was implemented to accumulate and interpolate the emerging solution history inside the solver, to facilitate regulation delays. All regulation input parameter values were taken from Ursino [24]. The mechanical model parameters are declared in Table 1.

#### 3.1 Local sensitivity analysis

The results of the LSA of the unregulated model are presented in Figure 4. To facilitate comparison, the unregulated system heart period, contractility and SVR were chosen to produce outputs close to the regulated equivalent ( $\tau_0 = 0.58$ ,  $E_{LVmax} = 2.48$ ,  $R_{sys} = 2.386$ ). Two heatmaps are presented for  $\pm 5\%$  and  $\pm 10\%$  perturbation of the model inputs. Despite the highly non-linear character of the model, these results show a similar pattern. In case of the cardiac output, the

most influential parameter in both cases is the heart period, but it is not highly influential on the other outputs. The least influential parameters are venous compliance and aortic valve resistance; mitral valve resistance is more important (than aortic) which may point to the significance of diastolic filling. The arterial compliance is much more significant than venous compliance.

The LSA results for the CV system with regulation are presented in Figure 5. As in the case of the un-regulated model, two heatmaps are presented, corresponding to a  $\pm 5\%$  and  $\pm 10\%$  perturbation of the model inputs. Again, despite the highly non-linear character of the model, these results show a similar pattern. In general, mechanical model inputs are more influential than regulation model inputs. Applying regulation does not significantly change the relative importance of the CV parameters. Unsurprisingly, the impact of the heart period on the cardiac output is more visible than in the unregulated system and the most influential control model factor is the set-point, ( $P_n$ ). There is higher sensitivity on parameters bounding neural activity ( $f_{min}$ ,  $f_{max}$ ,  $f_{es,0}$ ,  $f_{es,min}$ ,  $f_{ev,0}$ ,  $f_{ev,\infty}$ ) compared with rate parameters ( $k_a$ ,  $k_{es}$ ,  $k_{ev}$ ). Cardiac output is dominated by elastance parameters ( $E_{LVmin}$ ,  $E_{LVmax}$ ) and the heart period.

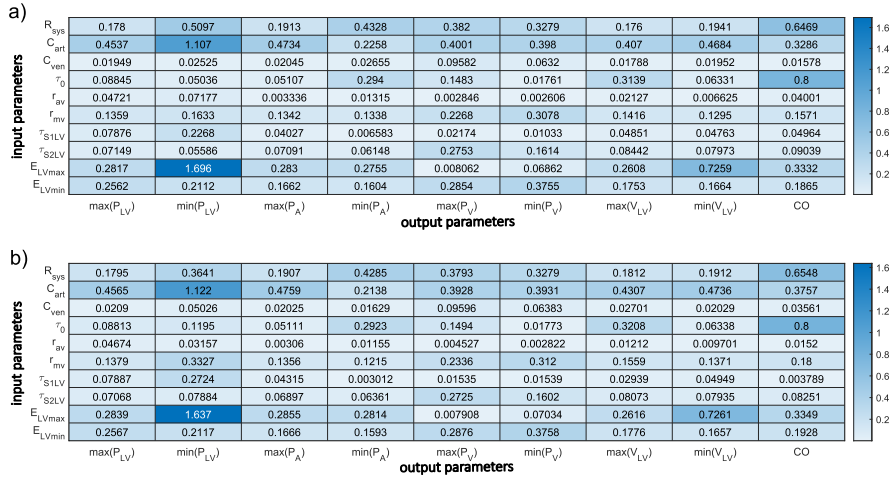


**Fig. 4.** Heatmaps of the local relative sensitivities of the unregulated base mechanical model, in figure 2, with parameters perturbed by a)  $\pm 5\%$ ; b)  $\pm 10\%$ . The unregulated model was parameterised to generate outputs close to the regulated equivalent in figure 5. The chosen model outputs were for these tabulations, maximum and minimum pressures (left ventricular:  $P_{LV}$ , arterial:  $P_A$  and venous:  $P_V$ ), maximum and minimum left ventricular volume ( $V_{LV}$ ) and cardiac output ( $CO$ ).

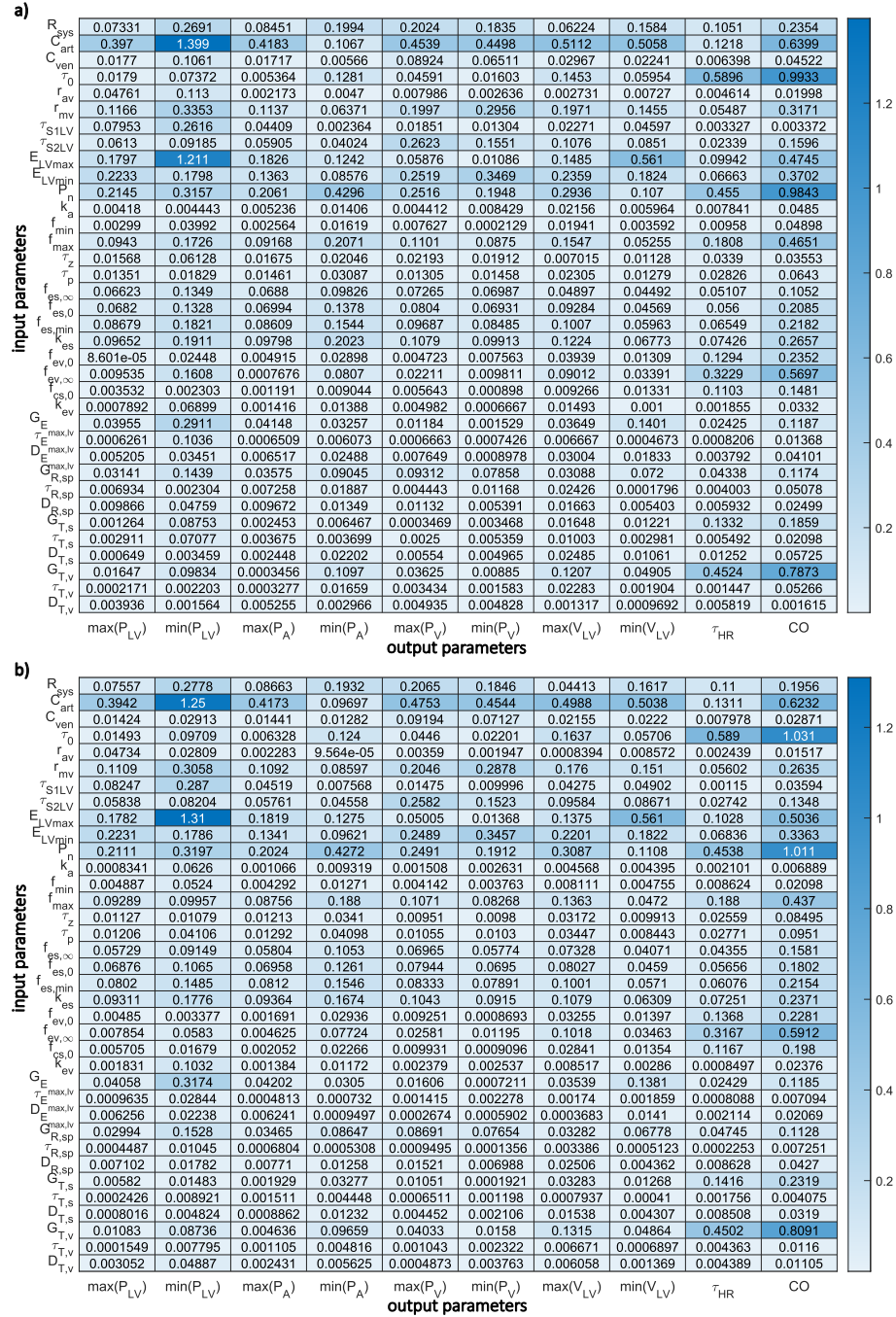


**Fig. 5.** Heatmap of the local relative sensitivities of the closed-loop, regulated model defined in figures 1 and 2, with parameters perturbed by  $\pm 5\%$  and  $\pm 10\%$ . The chosen model outputs were for these tabulations, maximum and minimum pressures (left ventricular:  $P_{LV}$ , arterial:  $P_A$  and venous:  $P_V$ ), maximum and minimum left ventricular volume ( $V_{LV}$ ), cardiac output ( $CO$ ) and heart period  $\tau_{HR}$ .



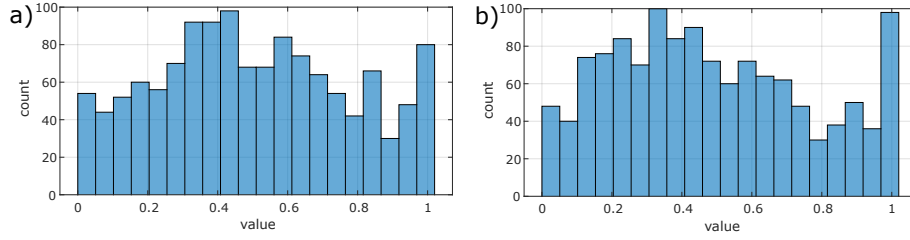


**Fig. 7.** The distribution of the orthogonality in the closed-loop regulated model defined in figures 1 and 2, with parameters perturbed by a)  $\pm 5\%$ ; b)  $\pm 10\%$ . These are the distributions of the  $d_{i,j}, i \leq j$ , i.e., the elements of Fisher information,  $\mathbf{F}$ .

## 4 Discussion

The LSA of the baroreflex model of Ursino [24] performed here is, to our knowledge, the first on a closed-loop model. Our model is a faithful representation of the Ursino model and does not implement averaging of the regulatory signal over a cardiac cycle. We also present the corresponding LSA of a *shadow*, unregulated system, to provide context.

The overall distribution of the LSA heatmap is similar for both regulated and unregulated models and for results for input perturbations at  $\pm 5\%$  and  $\pm 10\%$ . This consistency supports the tentative conclusion that our results in Figures 4 and 5 are truly characteristic of the system. However, the changes in the numerical values of the relative sensitivities between Figures 4 and 5 suggest non-linear interactions and the need for a global sensitivity analysis.

The purpose of the present LSA and orthogonality analysis is to expose the effect of regulation in a tractable way, by comparing the LSA of equivalent regulated and unregulated models in Figures 4 and 5. Clearly, mechanical CV model inputs are more generally influential than regulation factors, with the exception of the system set-point. Equally surprising is the persistence of the pattern in mechanical model sensitivities, as we pass from the unregulated to the regulated system. On the other hand, comparing Figures 4 and 5, the regulation is seen to suppress relative sensitivity of mechanical input factors - at least for the studied outputs. Notable exceptions include the influence of initial heart period on cardiac output (which might be anticipated) and the influence of arterial compliance on LV pressure.

The qualitative trends and connections from LSA provide tentative verification of Ursino's algorithm, combined with a single ventricle model of the systemic circulation. The response studied here represents an individual at rest, without additional loading applied to the CV system. One expects vagal activity to dominate cardiac output and this is apparent in e.g. the influence of the vagal gain  $G_{T,v}$  there. Put another way, the influence of vagal control on heart period,  $\tau_{HR}$ , and hence cardiac output, is significantly greater than the corresponding sympathetic control.

In Figure 7, the spread of sensitivity vector orthogonality indices  $d_{i,j}$  is more uniform than in the non-regulated equivalent system reported in [21]. It is unlikely that this is due to any shift between mechanical factors, rather the distribution shifts are likely due to the inclusion, in the statistics, of a large number of new regulation input factors.

## 5 Conclusions and further work

We have successfully implemented and tested, within closed-loop operation, the baroreflex regulation model proposed by Ursino [24] *without any algorithmic extensions* e.g. control signal cardiac cycle averaging, reporting LSA and orthogonality results. We are able to conclude, on the basis of our results, that explicit averaging of control signals is not a necessary component of a baroreflex model. Extension of this approach to compare these results with cycle-averaging of control signals, as discussed by other authors is of interest and will be considered in future work, particularly to explore the influence of cycle averaging on (i) system response and stability and (ii) computational time.

The coupled CV mechanical model used in this work is intentionally simple. Extension to include a four chamber cardiac model, the pulmonary circulation and venous tone regulation is tractable using the current approach.

A crucial feature of the physiological baroreflex is the phenomena of neuronal adaptation, which was also neglected here. The time-varying sensitivity of neurons will be included in future work to examine how this influences system sensitivity values.

LSA, combined with orthogonality analysis, provides the first tranche of information for model personalisation which is a fundamental requirement for all useful digital twins. It is essential, in even moderately complicated models, where a reduction of model inputs (a so-called *model reduction*) is necessary to bring about the decrease of computational cost necessary for a plausible global sensitivity analysis (GSA); put another way LSA is the accepted prelude to the much more costly, variance-based GSA [20], which captures non-linear interactions between inputs, and characterises only the model (in contradistinction to the model *and* its operating point), which we currently have in hand.

**Acknowledgments.** The publication was created within the project of the Ministry of Science and Higher Education "Support for the activity of Centers of Excellence established in Poland under Horizon 2020" on the basis of the contract number MEiN/2023/DIR/3796. This project has received funding from the European Union's Horizon 2020 research and innovation programme under grant agreement No 857533. This publication is supported by Sano project carried out within the International Research Agendas programme of the Foundation for Polish Science, co-financed by the European Union under the European Regional Development Fund.

**Disclosure of Interests.** The authors have no competing interests to declare that are relevant to the content of this article.

## References

1. Beccia, F., Causio, F., Farina, S., Savoia, C., Osti, T., Di Marcantonio, M., Morsella, A., Cadeddu, C., Ricciardi, W., Boccia, S.: Personalised Medicine in shaping sustainable healthcare: a Delphi survey within the IC2PerMed project. *European Journal of Public Health* **32**(Supplement 3), ckac129.429 (10 2022). <https://doi.org/10.1093/eurpub/ckac129.429>
2. Benarroch, E.: The arterial baroreflex functional organization and involvement in neurologic disease. *Neurology* **71**, 1733–8 (12 2008). <https://doi.org/10.1212/01.wnl.0000335246.93495.92>
3. Björdalsbakke, N.L., Sturdy, J.T., Hose, D.R., Hellevik, L.R.: Parameter estimation for closed-loop lumped parameter models of the systemic circulation using synthetic data. *Mathematical Biosciences* **343**, 108731 (2022). <https://doi.org/https://doi.org/10.1016/j.mbs.2021.108731>, <https://www.sciencedirect.com/science/article/pii/S002555642100136X>
4. De Boer, R.: Beat-to-beat blood-pressure fluctuations and heart-rate variability in man: physiological relationships, analysis techniques and a simple model. Ph.D. thesis (12 1985)
5. Gee, M., Lenhoff, A., Schwaber, J., Ogunnaike, B., Vadigepalli, R.: Closed-loop modeling of central and intrinsic cardiac nervous system circuits underlying cardiovascular control. *AIChE Journal* **69** (01 2023). <https://doi.org/10.1002/aic.18033>
6. Harris, D.M.: Regulation of Arterial Pressure, Mohrman and Heller’s Cardiovascular Physiology, 10th Edition. McGraw Hill, New York, NY (2023), [accessmedicine.mhmedical.com/content.aspx?aid=1200684113](https://accessmedicine.mhmedical.com/content.aspx?aid=1200684113)
7. Heldt, T.: Computational Models of Cardiovascular Response to Orthostatic Stress. Ph.D. thesis (2004)
8. Heldt, T., Shim, E., Kamm, R., Mark, R.: Computational modeling of cardiovascular response to orthostatic stress. *Journal of applied physiology* (Bethesda, Md. : 1985) **92**, 1239–54 (04 2002). <https://doi.org/10.1152/jappphysiol.00241.2001>
9. Jacobs, O.: Introduction to Control Theory. Oxford Science Publ, Oxford University Press (1993), <https://books.google.pl/books?id=df8pAQAAMAAJ>
10. Kamoi, S., Docherty, P., Squire, D., Revie, J., Chiew, Y.S., Desai, T., Shaw, G., Chase, J.: Continuous stroke volume estimation from aortic pressure using zero dimensional cardiovascular model: Proof of concept study from porcine experiments. *PloS one* **9**, e102476 (07 2014). <https://doi.org/10.1371/journal.pone.0102476>
11. Kawel-Boehm, N., Maceira, A., Valsangiacomo-Buechel, E.R., Vogel-Claussen, J., Turkbey, E.B., Williams, R., Plein, S., Tee, M., Eng, J., Bluemke, D.A.: Normal values for cardiovascular magnetic resonance in adults and children. *Journal of Cardiovascular Magnetic Resonance* **17**(1), 1–33 (2015)
12. Korakianitis, T., Shi, Y.: A concentrated parameter model for the human cardiovascular system including heart valve dynamics and atrioventricular interaction. *Medical engineering & physics* **28**, 613–28 (10 2006). <https://doi.org/10.1016/j.medengphy.2005.10.004>
13. Mackenzie, J.A.: A 1D model for the pulmonary and coronary circulation accounting for time-varying external pressure. Ph.D. thesis, University of Glasgow (2021)
14. Olsen, C.H., Ottesen, J.T., Smith, R.C., Olufsen, M.S.: Parameter subset selection techniques for problems in mathematical biology. *Biological cybernetics* **113**, 121–138 (2019)
15. Otta, M., Halliday, I., Tsui, J., Lim, C., Struzik, Z., Narracott, A.: Sensitivity analysis of a model of lower limb haemodynamics (01 2022). [https://doi.org/\\$10.1007/978-3-031-08757-8\\_7\\$](https://doi.org/$10.1007/978-3-031-08757-8_7$)

16. Ottesen, J.T., Mehlsen, J., Olufsen, M.S.: Structural correlation method for model reduction and practical estimation of patient specific parameters illustrated on heart rate regulation. *Mathematical Biosciences* **257**, 50–59 (2014). <https://doi.org/10.1016/j.mbs.2014.07.003>, <https://www.sciencedirect.com/science/article/pii/S0025556414001369>
17. Ottesen, J., Olufsen, M., Larsen, J.: *Applied Mathematical Models in Human Physiology*. Mathematical Modeling and Computation, Society for Industrial and Applied Mathematics (SIAM, 3600 Market Street, Floor 6, Philadelphia, PA 19104) (2004), <https://books.google.pl/books?id=EeNBWyrG-RYC>
18. Park, J.H., Gorky, J., Ogunnaike, B., Vadigepalli, R., Schwaber, J.S.: Investigating the effects of brainstem neuronal adaptation on cardiovascular homeostasis. *Front. Neurosci.* **14**, 470 (May 2020). <https://doi.org/10.3389/fnins.2020.00470>
19. Sala, L., Gelse, N., Joosten, A., Vibert, E., Vignon-Clementel, I.: Sensitivity analysis of a mathematical model simulating the post-hepatectomy hemodynamics response. *Annals of Biomedical Engineering* **51**(1), 270–289 (2023)
20. Saltelli, A., Ratto, M., Andres, T., Campolongo, F., Cariboni, J., Gatelli, D., Saisana, M., Tarantola, S.: *Global sensitivity analysis: the primer*. John Wiley & Sons (2008)
21. Saxton, H., Xu, X., Halliday, I., Schenkel, T.: New perspectives on sensitivity and identifiability analysis using the unscented kalman filter (06 2023)
22. Shi, Y., Lawford, P., Hose, R.: Review of zero-d and 1-d models of blood flow in the cardiovascular system. *Biomedical engineering online* **10**, 33 (04 2011). <https://doi.org/10.1186/1475-925X-10-33>
23. Simaan, M.A., Faragallah, G., Wang, Y., Divo, E.: Left ventricular assist devices: Engineering design considerations. In: Reyes, G. (ed.) *New Aspects of Ventricular Assist Devices*, chap. 2. IntechOpen, Rijeka (2011). <https://doi.org/10.5772/24485>
24. Ursino, M.: Interaction between carotid baroregulation and the pulsating heart: A mathematical model. *The American journal of physiology* **275**, H1733–47 (12 1998). <https://doi.org/10.1152/ajpheart.1998.275.5.H1733>
25. Vicente, A., Ballensiefen, W., Jönsson, J.I.: How personalised medicine will transform healthcare by 2030: the icpermed vision. *Journal of Translational Medicine* **18** (12 2020). <https://doi.org/10.1186/s12967-020-02316-w>
26. Zucker, M., Kagan, G., Adi, N., Ronel, I., Matot, I., Zac, L., Goren, O.: Changes in mean systemic filling pressure as an estimate of hemodynamic response to anesthesia induction using propofol. *BMC Anesthesiology* **22** (07 2022). <https://doi.org/10.1186/s12871-022-01773-8>